AURORAL SPORADIC E AND ITS RELATIONSHIP WITH VISUAL AURORA

D. C. NORTH *and* M. J. JARVIS

British Antarctic Survey, Natural Environment Research Council, High Cross, Madingley Road, Cambridge CB3 0ET, UK

ABSTRACT. The spatial and temporal correlation between discrete auroral forms and the apparently closely related ionospheric irregularities signified by auroral sporadic E (Es-a) traces on ionograms has been investigated. This has been achieved at Halley, Antarctica (76° S, 27° W, L = 4.2) by combining the echo-location capability of the Advanced Ionospheric Sounder (AIS) with photographic auroral data from a co-located All-Sky Camera (ASC); they provide data both inside and outside the auroral oval. The results of detailed analysis of data from 1985 have been combined with auroral and ionospheric data from 1961 and 1958.

It is shown that Es-a is basically a night-time phenomenon which, although closely related to discrete auroral forms, shows no one-to-one spatial relationship. It is further shown that there are two basic types (diffuse and stratified) having different diurnal and seasonal characteristics which can be identified on ionograms by their different frequency–height signatures. Diffuse auroral Es traces appear to be statistically linked to the proximity of the auroral oval and have an annual variation similar to that of discrete visual aurora. Stratified Es-a traces, while corresponding to periods of discrete aurora on a short-term basis, are predominantly a morningside phenomenon. They show no spatial relationship with the visible aurora.

It is suggested that, since the nature of diffuse and stratified Es-a traces are distinctly different, they should be separately identified when scaling ionograms.

INTRODUCTION

The correlation between the occurrence of radar echoes and visible aurorae has been studied by many observers using all-sky cameras (ASC) and a variety of ionospheric radars. The types of radar used to date range from ground-based, single-frequency HF radars (Shipstone, 1972) to airborne LF sweep frequency radars (Whalen and others, 1971). This paper discusses observations in which a digital ionosonde with direction-finding capabilities and a co-located ASC have been used to examine correlations between the two phenomena. It investigates the relationship between visible aurorae and auroral Es-a. This is a particular class of radio echo traditionally included in the Sporadic E (Es) classification – a term applied to additional ionization at normal E region heights between 95 km and 180 km which shows erratic temporal behaviour.

The classification of sporadic E forms an important contribution to reduced ionospheric data from ionospheric observatories since it is an indication of charged particle bombardment, plasma instabilities, wind shear or other phenomena present at the time of sounding. In the *Handbook of ionogram reduction and interpretation: UAG 23-A* (Piggott and Rawer, 1978), eleven standard Es types are identified, one of these being referred to as auroral Es (Es-a) and described in the following way: *All types of very diffuse (spread) traces are combined in auroral Es. These can extend over several hundred kilometres of virtual height. Typical patterns show a flat or slowly rising bottom edge, with stratified traces in it which vary rapidly with time.* Thus the broad classification of auroral Es includes many types of sporadic E which have ionogram signatures that are often quite different in nature and consequently likely to be different in cause.

Standard hourly ionogram scaling has been maintained at Halley, Antarctica (76° S, 27° W, L = 4.2) almost continuously (excluding 1959, 1962, 1981) since the International Geophysical Year of 1957. More recently, the deployment of the AIS (Grubb, 1979) at this station (Dudeney, 1981) has allowed more detailed information on auroral Es to be obtained. This paper utilizes the additional information that the AIS provides over the conventional ionosonde such as echo-location, line of sight Doppler velocity, and polarization sense of the echo (Wright and Pitteway, 1979) to present the diurnal and seasonal changes in the various auroral Es types, and discusses their relationship with variations in the discrete visible aurorae observed from the station using an all-sky camera.

Diurnal and Annual Variation in the Occurrence of Auroral Sporadic E

In order to achieve a detailed analysis of the diurnal and annual variation in the occurrence of auroral Es, additional routine scaling rules were introduced to hourly ionogram reduction during 1985. It is data from that year which have been used as a basis for this paper.

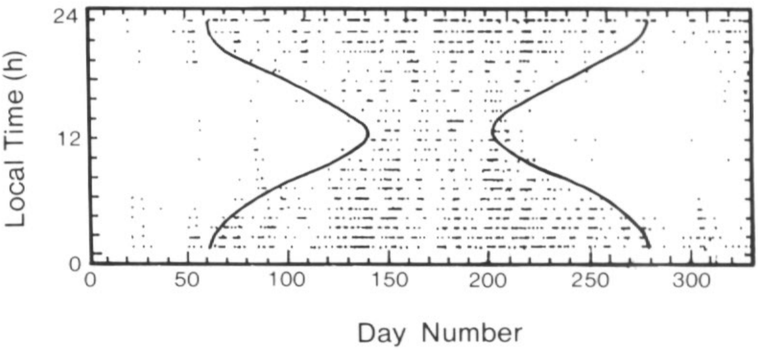

Fig. 1. Occurrence of all auroral sporadic E traces scaled in hourly ionograms during 1985. Each dot represents the occurrence of Es-a on one ionogram. The E region terminators are shown as solid lines.

A summary of the 1985 data is presented in Fig. 1; each data point represents an hour in which auroral Es was scaled and the area between the terminator lines shows times when the solar zenith angle exceeded 96° (effectively E region night-time). Approximately 85% of the observations of Es-a occur between the terminator boundaries which clearly suggests that the absence of solar radiation has a considerable influence on either the formation, lifetime or observation of the ionization features scaled as Es-a.

In Fig. 2 the diurnal variation in occurrence of this Es-a, normalized by the number of E region night-time observing hours, is given. It shows a background occurrence level of approximately 20% with a significant rise to about 45% two to three hours prior to local midnight. This higher level is maintained until four hours after local midnight after which it slowly decreases, reaching a minimum after midday.

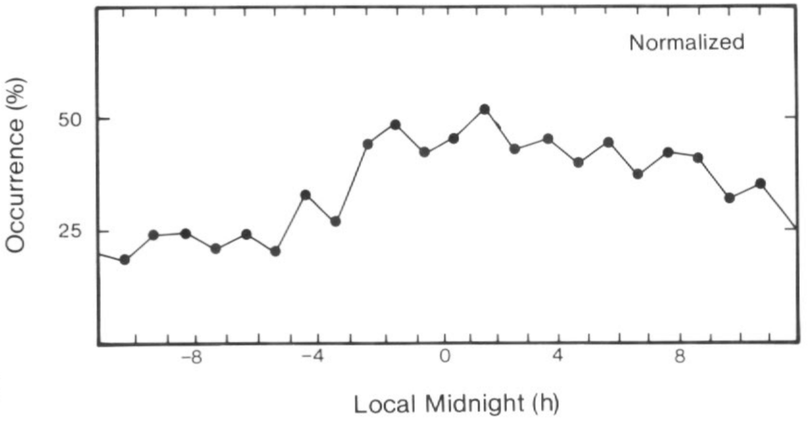

Fig. 2. Diurnal variation of the occurrence of all auroral Es traces for 1985 normalized by the number of E region night-time observing hours.

Comparisons are made in Figs 3 and 4 between the occurrence of auroral Es data obtained using the AIS during 1985 and data taken from a conventional ionosonde, the Union Radio Mk 2, during 1958 as part of the International Geophysical Year expedition (Bellchambers and others, 1962). These datasets were both recorded at Halley and represent contrasting periods in the solar cycle, 1958 being close to sunspot maximum and 1985 approaching sunspot minimum. Note that the two ionosondes have different characteristics and that the scaling of hourly ionograms is subjective, the scaling conventions for Es parameters inevitably being based on compromise; there exist many borderline situations in which a weak trace could be scaled by one operator and ignored by another. Thus, although the datasets are presented in the same format, only the gross differences are significant.

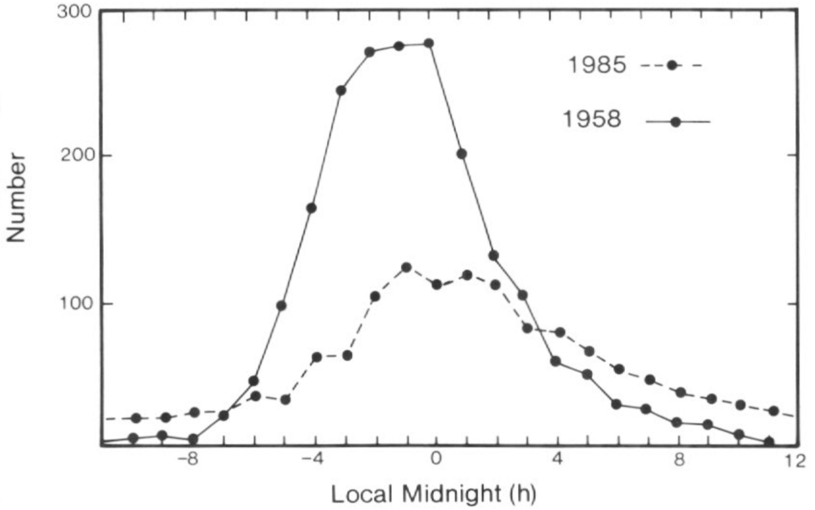

Fig. 3. A comparison of the diurnal variation in the occurrence of Es-a for 1958 (sunspot maximum) and 1985 (approaching sunspot minimum); unlike the data shown in Fig. 2, the data here are not normalized.

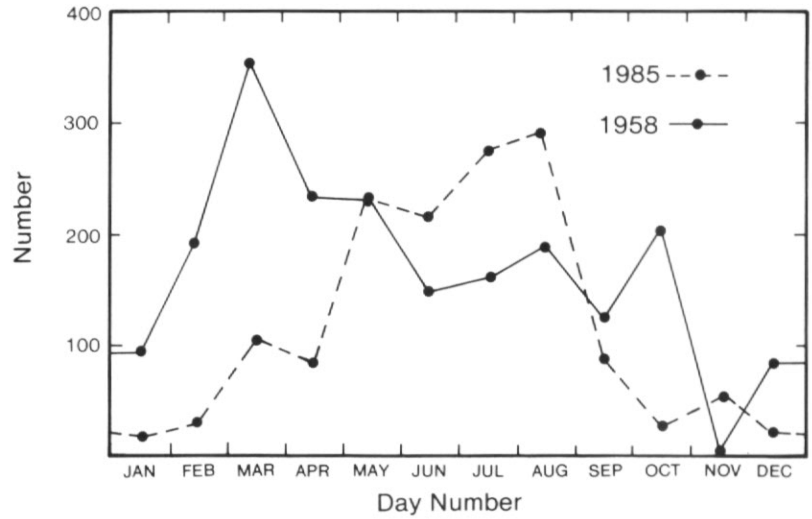

Fig. 4. A comparison of the seasonal variation in occurrence of Es-a for 1958 and 1985.

The diurnal occurrence of Es-a (Fig. 3) shows the same basic variation for both years, peaking just before local midnight and presenting a broad minimum about midday. To facilitate comparison between the two datasets, the 1985 data have not been normalized and Figs 2 and 3 should therefore not be directly compared. The larger amplitude of the 1958 data about local midnight may be explained by increased solar activity during this year, moving the auroral oval closer to a sub-auroral station more frequently. The mean Ap indices for 1958 and 1985 were 19.4 and 13.7 respectively.

Annual variations in the occurrence of Es-a (Fig. 4) are decidedly different. In 1985 the winter peak at solar minimum spans four months (May–August) while at solar maximum it spans eight months (March–October) reflecting an increase in occurrence of Es-a at the equinoxes. A double peak structure with a minimum in June (midwinter) is present in both years (see also Fig. 7). Although auroral sporadic E is frequently associated with ionospherically disturbed periods (Rishbeth and Garriott 1969), the large number of Es-a traces at or near the equinoxes in 1958 do not, however, coincide with any significant change in magnetic activity.

Classification of Auroral Es Types

Figs 1–4 contain all the data during 1985 scaled as Es-a. As noted in the introduction, this category includes several varied ionogram signatures. In order to investigate the physical nature of the processes leading to each type of ionogram signature, each occurrence of auroral Es was classified into one of a number of groups according to its appearance. The three main groups were termed diffuse, stratified and mixed and are mutually exclusive; the remaining categorizations are subsets used to describe further the three main groups. A detailed description follows.

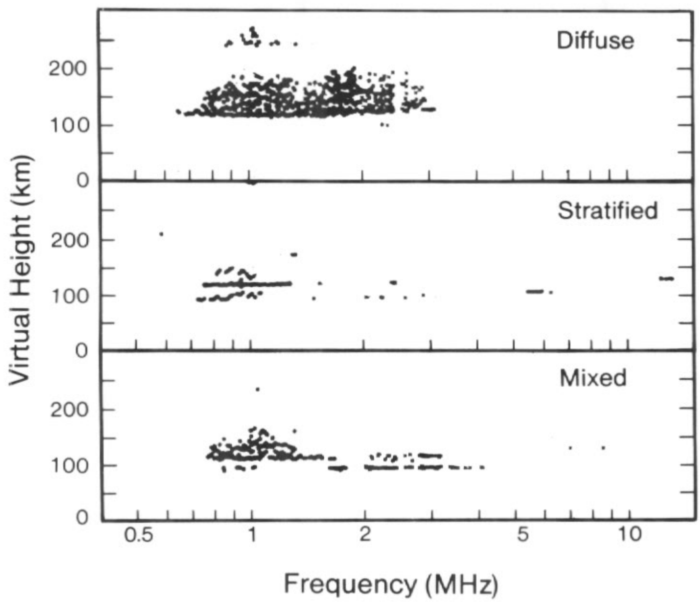

Fig. 5. Typical examples of the three main Es-a types (diffuse, stratified and mixed) observed with the AIS.

Groups

Diffuse (Fig. 5, top) describes a trace spread both in frequency and in range; it shows no internal structure and is, in fact, the most common of all classifications used.

Stratified (Fig. 5, centre) describes one or more distinct traces showing small increases of virtual range with increasing frequency giving the trace a stratified appearance. The main distinction between this and those non-auroral traces scaled as 'flat' (i.e. a sporadic E layer with a stratified appearance: UAG 23) is that the majority of the stratified class are observed at much higher frequencies and do not show the consistency in multiple order traces which, when present, indicates an overhead trace. Stratified traces have been observed to extend up to, and probably exceed, the maximum frequency (30 MHz) of the ionosonde. More than one stratified trace can be present in one ionogram.

Mixed (Fig. 5, bottom) is a combination of the previous two types and has the appearance of quasi-horizontal lines embedded within a diffuse cloud of echoes. If both stratified and diffuse traces occur but can be easily separated, normally because they occur on different parts of the ionogram, the only one to be scaled would be the trace identified by the internationally agreed scaling rules (Piggott and Rawer, 1978).

Subsets

Low frequency. Used if the mean frequency of the trace is less than ~ 1 MHz.

High and very high frequency. Used if the trace exceeds 3 and 4 MHz respectively.

More than one group present. Used when there is more than one trace which can be referred to as auroral Es.

Extensive. Used when a trace has unusually large spread in frequency or height (e.g. greater than 7 MHz or 400 km).

Classical. This applies to diffuse echoes only and refers to the shape of the trace. The lower edge of the trace is well defined and rises slowly in virtual height with increasing frequency. The inside edge is also well defined but rises rapidly with increasing frequency. This is the type that most often appears in textbooks.

Weak. Used for borderline cases when received echoes are only just strong enough to be treated.

Table I gives the total number of occasions for which each classification was recorded on hourly ionograms during 1985. Also shown are the occurrence of each type as a percentage of all hourly ionograms and as a percentage of all hourly ionograms containing auroral Es.

Table I. Number of Es-a classifications

	Total	*% of all*	*% of Es-a*
Group classifications			
Diffuse	1103	13.0	68.0
Stratified	308	4.6	19.0
Mixed	251	2.9	15.4
Subset classifications			
Low frequency	242	2.8	14.9
High frequency	35	0.4	2.1
Very high frequency	17	0.2	1.0
Classical	147	1.7	9.0
Weak	395	4.6	24.3
Extensive	129	1.5	7.9
More than one group present	173	2.0	10.6

Occurrence Characteristics of Diffuse and Stratified Es-a

The different occurrence characteristics of the *diffuse* and *stratified* types have been studied by comparing them on three different timescales: diurnally, annually and minute-by-minute.

Fig. 6 (top) shows stratified data recorded through 1985 for each hour relative to local midnight. There is a significant rise in occurrence close to local midnight followed by a post-midnight broad peak. The variation in occurrence throughout the day is relatively small (approximate ratio of 2:1, midnight:midday). In contrast, the same statistics presented for diffuse (Fig. 6, bottom) show a strong local time dependence, peaking two hours before midnight with a midnight:midday ratio of 20:1, an order of magnitude greater than in the stratified case. This suggests a quite different production mechanism. The shaded region in the figures represents the mixed classification. Unlike Fig. 2, Fig. 6 is not normalized for E region night-time. This is for comparison with datasets published previously which have likewise not been normalized.

Markedly different characteristics between stratified and diffuse types are also seen in the annual occurrence rate (Fig. 7). The centre panel shows the occurrence of stratified traces to have an upward trend through the austral winter until early September when there is a rapid drop in less than one month to a low summer-time level. Variation of the occurrence of diffuse traces (bottom panel) exhibits a more symmetrical pattern, with local maxima near days 140 and 210.

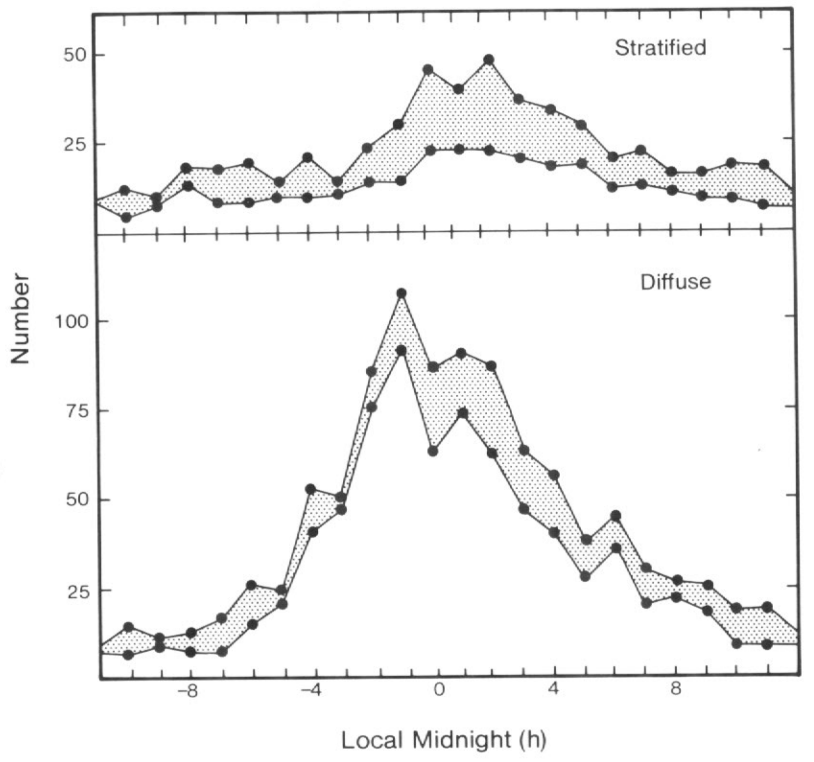

Fig. 6. Diurnal variations of the occurrence of stratified and diffuse Es-a (the shaded regions represent the occurrence of 'mixed' Es-a – see text).

As is evident in the example shown in Fig. 5, diffuse Es-a echoes often, but not always, come from a greater virtual height than stratified Es-a traces. This does not necessarily imply that the reflection region is at a higher altitude, since echo-location with the AIS often shows the echoes to be received obliquely.

Diurnal and seasonal variations have also been plotted for each of the subgroups (not reproduced). The following characteristics were noted:

(1) The occurrence of *low frequency* class traces is highly variable throughout the year, but shows a diurnal variation peaking about local midnight with a minimum at midday – possibly owing to screening of these layers by the normal E during the day.

(2) The *more than one trace present* class shows annual occurrence characteristics similar to those of the diffuse class, with peaks on days 160 and 215. The diurnal occurrence increases in an exponential fashion to a sharp peak one hour before local midnight then falls approximately linearly to zero at noon.

(3) The *extensive* class is characterized by a steady diurnal variation with broad peaks at local midnight and midday. However, as seen from Table I, the number of scaled extensive types is relatively small.

(4) The *classical* class shows similar characteristics to that of the 'More Than One Group' class. It has a sharp peak an hour before local midnight and its occurrence is highly variable throughout the year.

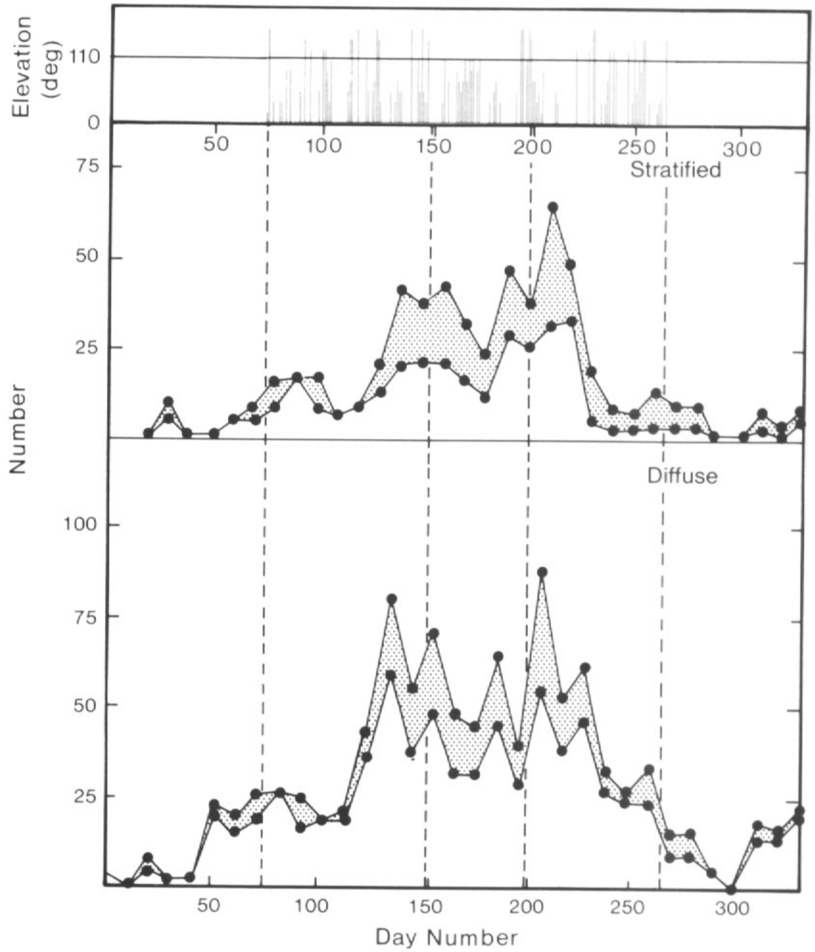

Fig. 7. Annual variation of the occurrence of stratified and diffuse Es-a for 1985 (the shaded regions represent the occurrence of 'mixed' Es-a – see text). The upper panel shows the maximum elevation of discrete auroral forms observed during clear intervals in each 24-hour period during 15 March–30 September (from Blackie, 1961).

Statistical Comparison of Es Types with Visible Aurora Data

The two main classes of Es-a, diffuse and stratified, might be expected to correspond to different signatures in the all-sky camera data. Ideally, for a statistical study, Es-a data would be compared with records of visible aurora at Halley during the same year. The all-sky camera programme run during 1985 was based on a campaign philosophy thus providing exceptionlly good datasets for one-to-one comparisons with ionospheric data for short periods, but rendering statistical use, for seasonal and diurnal comparisons, impossible. Blackie (1961) showed, after considering the changes in all-sky camera data through 5 years (1956–60), that, apart from the slight tendency for large active displays to occur more frequently close to the equinoxes, there were no significant seasonal variations of auroral occurrence at Halley. He did, however, find that the time of maximum occurrence of visible aurora through the night changed considerably from year to year, shifting towards the morning during periods of declining solar activity. This trend is apparent in the Es data (Fig. 3) with the night-time broad peak in the solar maximum year of 1958 occurring before that in 1985, a period of declining solar activity.

Consequently, it is reasonable, for statistical purposes, to compare the seasonal, but not the diurnal, variation of 1985 Es-a data with an earlier comprehensive study of all-sky camera data for 1960 (Blackie, 1961; Blundell, 1967). In Fig. 7, the upper panel shows the elevation of discrete auroral forms observed at Halley during the comprehensive observation programme between 15 March and 30 September 1960 (Blackie, 1961). Blackie's data only cover 'clear' (non-cloudy) nights and do not therefore represent a complete statistical picture. Each line extends to the maximum northerly extent in elevation above the southern geomagnetic horizon during each 24-hour period (midday–midday). The line at 110° represents the geomagnetic field line extending from the station into the magnetosphere; the extension of lines above this shows auroral forms equatorward of this field line. This plot confirms what is consistently observed from Halley, that the visible auroral season is characterized by two periods of high activity about a relatively quiet midwinter. This behaviour is more similar in shape to that of the diffuse Es-a than to that of the stratified.

One-to-One Examples

A series of 80 one-to-one comparisons were made from a sequence of all-sky camera photographs and ionograms taken at 5- and 1-minute intervals simultaneously over a period of four hours from Halley (18.54 LT to 22.26 LT on day 110, 1985). The photographs have a 10-second exposure time while an ionogram sounding from 400 kHz to 15 MHz takes approximately 40 s to complete, passing through 3 MHz at the start of the ASC photo. This sequence was taken during a period of high magnetic activity (local K indices 4 and 8); auroral forms appeared over the station and strong ionospheric reflections were received. Both preceding this sequence and following it, ionospheric blackout prevailed.

Of these 80 photographs, 27 have discrete auroral arcs within a cone described by an angle of 45° from the zenith. From inspection of the ionograms, no distinction can be made between occasions when discrete visible aurorae are present and those when no such forms are near the station, though they all contain characteristic oblique auroral Es traces (15 stratified, 5 diffuse and 7 mixed). In most cases, these are accompanied by overhead ionization mostly of the diffuse nature. All 80 would be scaled by international rules as totally blanketing auroral Es.

The Advanced Ionospheric Sounder, together with external analysis software (Dudeney and Jarvis, 1986), provides a sophisticated echo-location capability. Unfortunately, a fault in one receiver antenna during this sequence of 'rapid-fire' all-sky camera photographs prevented accurate location of the echoing points in the north–south plane. This particular dataset was still used for analysis, however, and since it provides the best examples of discrete auroral forms and simultaneous oblique ionospheric reflections, it is still possible to compare data in the east–west plane. An example showing typically poor correlation between the location of visible aurora and auroral Es is shown in Fig. 8 (top). The upper panel shows auroral intensity across the sky from the eastern to western horizon, averaged through ±100 km from Halley in the north–south plane at a height of 100 km. No allowance has been made for the Van Rhijn effect (Chamberlain, 1961). Ionospheric echoes for this time are shown in the bottom panel. It can be seen from the intensity profile that visible aurorae are present far to the east, far to the west and at a zenith angle of 35° in the

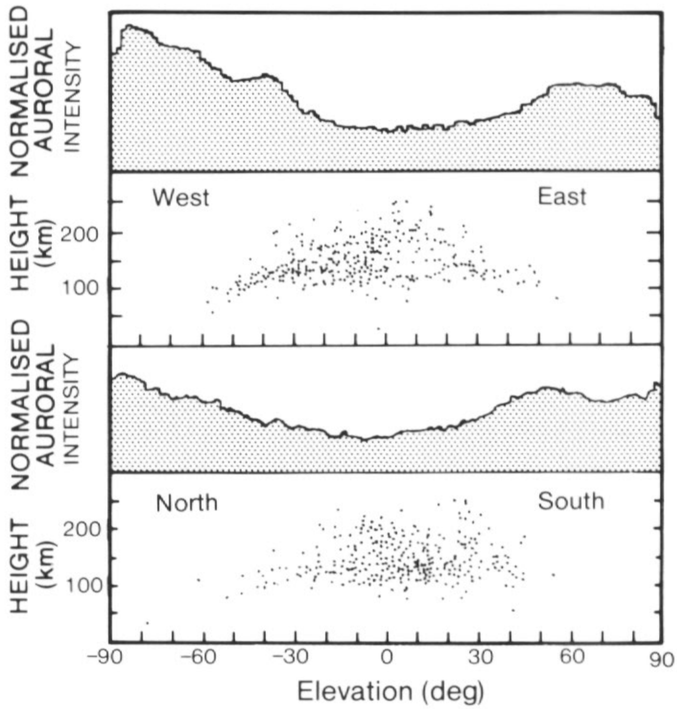

Fig. 8. Profiles of radio echoes received over Halley in the west–east and north–south planes, together with the respective intensity profiles of auroral forms.

west direction (indicated by the local maximum). No corresponding ionospheric features are observed by the AIS.

Data from other periods in which the echo-location information is available in both planes have been analysed using the same technique. A typical example is given in Fig. 8 (bottom). Again they show, without doubt, that given the conditions in which discrete aurora is within range of the ionosonde, no corresponding echoes are located near it. Fig. 9 shows the best correlation between the two phenomena after looking at well over one hundred cases.

Discussion

It has been shown (Fig. 1) that auroral Es is predominantly observed in the absence of direct solar radiation. One reason for this may be that incident radiation on the E-region ionosphere greatly increases the background ionization density in which the irregularities are formed. Firstly, this will decrease the ratio of irregularity to background concentration. The maximum plasma frequency for an illuminated E-region at Halley is usually in the range of 2–3 MHz and 18% of all auroral Es traces scaled were below 3 MHz; by comparison, the night-time E-region maximum background plasma frequency might be expected to be well below 1 MHz. Hence, this represents a 15-fold decrease in the ratio of irregularity to background electron density from night to day. Secondly, it will change the refractive index of the ionization through which the radio waves pass. Assuming that the irregularities are field-aligned, this change in refractive index could be sufficient to refract the wave away from the

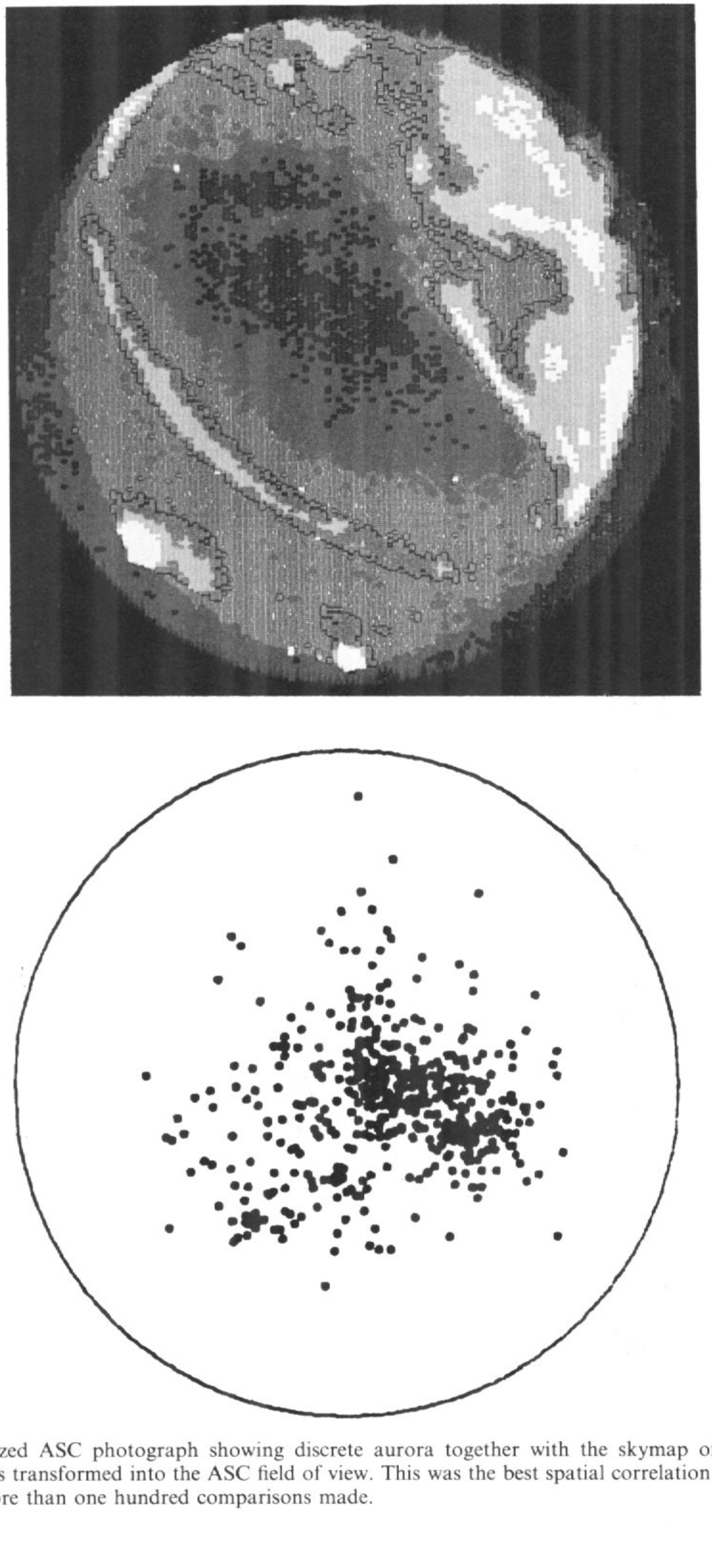

Fig. 9. Digitized ASC photograph showing discrete aurora together with the skymap of ionospheric echoes transformed into the ASC field of view. This was the best spatial correlation achieved out of more than one hundred comparisons made.

orthogonal reflection situation required (Dudeney and Rodger, 1985) for their observation.

A second reason for the relative absence of auroral Es under solar illumination may be that there is a significant reduction in the lifetime of the plasma enhancements due to the increase in ionospheric conductivity and hence more rapid redistribution of charge (Vickrey and Kelly, 1982).

The statistical study of Es-a occurrence has shown that there is a significant diurnal variation even when the data are normalized for night-time conditions only. This is possibly due to the influence of the auroral oval which, by virtue of the geomagnetic location of Halley, is closest to the station between local midnight and 0200 LT (Akasofu, 1978). The contribution to the occurrence of auroral Es that might be associated with the eccentric rotation of the auroral oval about the geographic pole would therefore exaggerate the variations shown in Fig. 1; it does not explain the close fit of data points to the terminator lines.

There also exists the background occurrence of 20% which persists throughout the 60 days around midwinter when the sun never rises at E-region heights or below. Consequently, the E-region is in continuous darkness, with production of Es-a even around noon when the auroral oval is far from the station. This may suggest that some irregularities scaled as auroral Es are, in fact, formed by metallic ions or perhaps scattered solar Lyman alpha radiation.

When the Es-a data are classified into stratified and diffuse types, it is the diffuse type which shows stronger links with the position of the auroral oval. This implies that there may be a common mechanism responsible both for the production of the irregularities resulting in diffuse Es-a and for the visible aurora. Observation has substantiated that active visual displays are accompanied by numerous Es-a traces. Indeed, Blundell (1967), using data from Halley, writes briefly on the association of aurora with the ionosphere. He considers the relationship between different auroral forms (active aurora, diffuse surfaces, homogeneous arcs, glows or flaming aurora) and the type of sporadic E observed during the same night. He concludes that active auroral forms are associated with the occurrence of blackout, auroral Es and slant Es (a rare, steadily rising diffuse trace) and, further, that when there is no aurora, or merely a glow, auroral Es and slant-type Es occur very infrequently.

No attempt is made in this paper to relate Es-a to the diffuse aurorae on a one-to-one basis since the relatively low intensity emissions associated with it are even more susceptible to poor observation conditions such as moonlight or thin cloud. However on the occasions when it is observed, without additional discrete auroral forms, the ionosphere is generally quiet with only occasional traces of auroral Es. The precipitation energy flux associated with diffuse aurorae has been observed to be much greater than that associated with discrete forms (with the exception of pulsating aurora) (Lyons and Fennell, 1986) so its effects cannot be ignored.

Many different combined radar and all-sky camera studies have examined the correlation between the location of radar echoes and those of visual aurorae. From these studies, many different conclusions have been drawn. For example, Little and others (1956), after summarizing much work using VHF radar echoes, concluded that the radio wave scatterers are closely associated in space and time with visual aurorae. However, they cited the aspect sensitivity at these frequencies to be such that echoes were rarely received at greater than 20° elevation. This low elevation sensitivity occurs because the ionospheric irregularities responsible for the backscatter of echoes are highly field-aligned. Lyon (1960), using a 48.2 MHz radar and an ASC at a remote site 500 km from the radar, found remarkable similarity between the diurnal variation of radar echoes and discrete aurora that he termed curls (arcs with a spiral discontinuity). In general, good spatial correlations are found between radar echoes and discrete aurora from equipment designed to receive distant echoes at low elevations. This is because (1) the condition for orthogonal reflection is more easily satisfied, and (2) the more distant the echoes the less accurate the echo-location and the more easily the term 'good correlation' may be applied. It is estimated that the AIS can provide echo-location accurate to within 10 km at 5 MHz for E-region heights (Jarvis and Dudeney, 1986), which is a considerable improvement on previous measurements for which the error was $\sim$ 30 km. Using the AIS, no spatial one-to-one correlations are observed. Unlike the VHF radars, the AIS predominantly sees auroral Es at high elevations within $\sim 60°$ of the zenith. This is due to directivity of the transmitting antenna and the relatively low frequencies and hence increased D-region absorption at more oblique incidence.

The relatively sharp increase in occurrence of the stratified auroral Es prior to midnight, the predominance in the morning hours and a fall-off to a minimum in the afternoon are suggestive of direct production by precipitation of energetic electrons injected from the plasma sheet and travelling eastwards around the Earth (Lyons and Fennell, 1986). Rodger and others (1983) have shown, in a study of Es under the mid-latitude trough, that thick and thin Es types occur predominantly before and after midnight respectively. One mechanism they proposed to explain this difference was the oppositely directed vertical motion of the plasma about magnetic midnight driven by the convection electric field. This mechanism may also explain, at least in part, the asymmetric occurrence of stratified auroral Es about midnight seen here.

From the examination of ionograms coincident with, preceding and following all-sky camera pictures, it has been shown than there is no one-to-one spatial correspondence between discrete auroral forms and stratified ionogram traces. Neither is the ionization a spatially coincident remnant or precursor of the auroral form. The poor correlation of the two phenomena is perhaps not surprising considering the time constants involved. The relaxation time for the excited atoms responsible for the visual aurora is a fraction of a second (for 557.7 nm oxygen radiation) but recombination times in the E region can be as long as one minute, thus the possibility of plasma transport must be considered. The short-term effect of a discrete auroral arc has been studied recently (Hapgood and Lanchester, 1986) using the EISCAT radar system (Rishbeth and Williams, 1985) and low light level TV cameras. During the passage of an extremely bright auroral arc through the radar beam, the ionization rate in the E region was observed to increase by at least 20-fold for one to two seconds and to decay back to its initial level in 10 seconds. By comparison, an ionogram takes 40 seconds to complete. They concluded that the sudden increase in electron concentration was caused by a narrow, intense electron beam associated with the bright arc. From (1983), using a single frequency, HF radar studied the movement of sporadic E regions at mid-latitudes. He concluded that the velocities for isolated clouds of Es vary from 20 to 100 m/s. At high latitudes much higher velocities might be expected.

Using echo-location and Doppler velocity measurements from the AIS it is evident from the analysis of individual ionograms with several stratified traces that their motion is often rapid and in different directions for different traces. This would make any consistent pattern of remaining ionization left in the wake of auroral arcs almost impossible to discern and could largely explain the long time scale correlation between visible auroral forms together with the lack of any short-term simultaneity.

Additionally, external influences such as wind shears or gravity waves and especially electric fields (Turunen and others, 1985) could move this newly formed plasma either from shapes unlikely to reflect radio waves to observable structures, or vertically redistribute it, seriously influencing the observed ionospheric signature.

Conclusions

(1) Auroral Es recorded at Halley is observed predominantly when the ionosphere is not directly illuminated by the sun and should therefore be considered to be a night-time phenomena.

(2) Auroral Es data normalized for E region night-time show a diurnal variation superposed on a background occurrence of approximately 20%, with a broad maximum centred about 0400 LT and a minimum near 1500 LT.

(3) The auroral-type sporadic E frequently observed in ionograms at mid- to high latitudes can generally be divided into two types. Stratified Es-a shows a small diurnal variation, an asymmetric seasonal occurrence and a lifetime of a few minutes or less; on occasions it exceeds 25 MHz. Diffuse Es-a shows a high dependence on local time, occurs approximately symmetrically about midwinter and is observed continuously over hours rather than minutes.

(4) Stratified Es-a observed using the AIS echo-location facility, is not spatially coincident with discrete auroral forms. Although visual arcs are often accompanied by numerous auroral Es traces not normally present when the aurora is distant, they appear to be neither a spatially coincident precursor nor a remnant of discrete aurora.

(5) The diurnal variation of stratified Es-a suggests a link with the plasma sheet as a source for an energetic electron precipitation flux or, alternatively, that the convection electric field plays a significant role in its formation or decay.

(6) The diurnal variation of diffuse Es-a suggests a strong link with the auroral oval.

(7) It is suggested that since the diffuse and stratified traces are clearly different in almost every way (i.e. timescale, diurnal and seasonal variations, maximum density and nature of reflecting feature) they should not be scaled under the global descriptor 'auroral Es' but should be separately identified.

Acknowledgements

The authors wish to thank members of the Geospace Research Group, in particular A. S. Rodger, for useful discussion and comment regarding this work, and also the AIS field engineers and other base personnel at Halley for maintaining and running the equipment.

Received 11 November 1987; accepted 25 January 1988

References

Akasofu, S.-I. 1978. *Antarctic Research Series*, **29**, 157–99.

Bellchambers, W. H., Barclay, L. W. *and* Piggott, W. R. 1962. The Royal Society IGY Expedition, Halley Bay, 1955–1959, **2**, 179.

Blackie, J. R. 1961. Analysis of auroral observations, Halley Bay 1960. *British Antarctic Survey Scientific Reports*, No. 40, 61 pp.

Blundell, G. 1967. Analysis of auroral observations, Halley Bay, 1961 and 1962. *British Antarctic Survey Scientific Reports*, No. 48, 72 pp.

Chamberlain, J. W. 1961. *Physics of the aurora and airglow*. New York, Academic Press.

Dudeney, J. R. 1981. The ionosphere – a view from the pole. *New Scientist*, **91**, 714–17.

Dudeney, J. R. *and* Jarvis, M. J. 1986. A simple graphical method for dealiasing digital ionosonde echo location data. *Radio Science*, **21**, 110–15.

Dudeney, J. R. *and* Rodger, A. S. 1985., Spatial structure of high latitude sporadic E. *Journal of Atmospheric and Terrestrial Physics*, **47**, 529–35.

FROM, W. R. 1983. Sporadic E movement followed with a pencil beam high-frequency radar. *Planetary and Space Science*, **31** (12), 1397–407.

GRUBB, R. N. 1979. The NOAA SEL HF radar system (ionospheric sounder). NOAA Technical Memo ERL SEL-55, National Oceanic and Atmospheric Administration, Boulder, Colorado.

HAPGOOD, M. A. *and* LANCHESTER, B. S. 1986. A narrow auroral arc observed with EISCAT. *Journal of Atmospheric and Terrestrial Physics*, **49**, 49–55.

JARVIS, M. J. *and* DUDENEY, J. R. 1986. Reduction of ambiguities in HF radar results through a revised receiving antenna array and sounding pattern. *Radio Science*, **21**, 151–8.

LITTLE, C. G., RAYTON, W. M. *and* ROOF, R. B. 1956. Review of ionospheric effects at VHF and UHF. *Proceedings of the Institute of Radio Engineers*, **44**, 992–1018.

LYON, G. F. 1960. The association of visible auroral forms with radar echoes. *Canadian Journal of Physics*, **38**, 385–9.

LYONS, L. R. *and* FENNELL, J. F. 1986. Characteristics of auroral electron precipitation on the morningside. *Journal of Geophysical Research*, **91**, 11 225–34.

PIGGOTT, W. R. *and* RAWER, K. 1978. *URSI Handbook of ionogram interpretation and reduction*, 2nd edition (revised). World Data Centre A, Washington. National Oceanic and Atmosphere Administration report UAG-23A.

RISHBETH, H. *and* GARRIOTT, O. K. 1969. *Introduction to ionospheric physics*. New York, Academic Press.

RISHBETH, H. *and* WILLIAMS, P. J. S. 1985. The EISCAT ionospheric radar: the system and its early results. *Quarterly Journal of the Royal Astronomical Society*, **26**, 478–512.

RODGER, A. S., MORRELL, C. *and* DUDENEY, J. R. 1983. Studies of sporadic E (Es) associated with the main ionospheric trough. *Radio Science*, **18**, 937–46.

SHIPSTONE, D. M. 1972. A study of the radio aurora and meteors at Halley Bay during the IQSY. *British Antarctic Survey Scientific Reports*, No. 74, 70 pp.

TURUNEN, T., SILEN, J., NYGREN, T. *and* JALONEN, L. 1985. Observation of a thin Es-layer by the EISCAT radar. *Planetary Space Sciences*, **33**, 1407–16.

VICKREY, J. F. *and* KELLY, C. K. 1982. The effects of a conducting E layer on classical F region cross-field plasma diffusion. *Journal of Geophysical Research*, **87**, 4461–8.

WHALEN, J. A., BUCHAU, J. *and* WAGNER, R. A. 1971. Airborne ionospheric and optical measurements of noontime aurora. *Journal of Atmospheric and Terrestrial Physics*, **33**, 661–78.

WRIGHT, J. W. *and* PITTEWAY, M. L. V. 1979. Real-time data acquisition and interpretation capabilities of the Dynasonde. 2. Determination of magnetoionic mode and echo location using a small spaced receiving array. *Radio Science*, **14**, 827–35.